Getting from sea to nurseries: Considering tidal dynamics of juvenile habitat distribution and connectivity in a highly modified estuarine riverscape

Maria Alp, Céline Le Pichon

Full title:

Getting from sea to nurseries: considering tidal dynamics of juvenile habitat distribution and connectivity in a highly-modified estuarine riverscape

Short title: Getting from sea to nurseries

Authors : Maria Alp[1,2], Céline Le Pichon[1]

Author affiliations:

[1] Université Paris-Saclay, INRAE, UR HYCAR, 1 rue Pierre-Gilles de Gennes, 92761, Antony, France

[2] INRAE, UR Riverly, 5 rue de la Doua, 69625, Villeurbanne, France

Corresponding author: Maria Alp, maria.alp@inrae.fr, +33 4 72 20 87 96.

Author contributions: MA and CLP contributed equally to study design and manuscript preparation. MA led the data preparation and least-cost modelling.

Abstract

Productive and ecologically highly valuable ecosystems, macrotidal estuaries are also characterised by complex habitat and connectivity dynamics driven by tidal and freshwater influence. Organisms living in these constantly changing systems have to match their movement patterns to the shifting habitat mosaic using available windows of connectivity to access habitat patches of interest. This appears particularly important for the juvenile stages of many fish species colonising shallow and intertidal areas of the estuaries as summer nurseries. We apply tools from landscape ecology to investigate the estuarine habitat and connectivity dynamics on the example of juvenile seabass (*Dicentrarchus labrax*). We test, under which conditions spatio-temporal bottlenecks to estuarine nursery colonisation may emerge for this species in a human-modified estuary. Combining a hydrodynamic model of the Seine estuary with remote-sensing data allows us to capture structural changes in habitat availability and connectivity at the estuarine scale and at a fine spatio-temporal resolution. With chronological least-cost modelling of successive tidal steps, we assess patterns of nursery accessibility and estimate tidal colonisation fronts for different mobility scenarios. We show that, at certain hydrological conditions, tidal water level variation causes local disruptions of habitat availability and connectivity, creating temporary bottlenecks for seabass juveniles' movement. Fish mobility appears determinant for their vulnerability to these connectivity disruptions. Our approach allows for quantitative assessment and visualisation of riverscape complexity related to tidal dynamics. It is applicable to other highly dynamic ecosystems, where the mobile nature of connectivity and habitats needs to be integrated into conservation and management planning.

Keywords: least-cost modelling, spatio-temporal hydrodynamics, functional connectivity, habitat patch dynamics, tidal cycle, dispersal, nursery habitats, Seine estuary, European seabass *Dicentrarchus labrax*

Manuscript highlights

- Tidal estuarine habitat distribution and connectivity change on an hourly scale
- Transient bottlenecks to movement emerge in estuaries with modified topography
- Juvenile fish sensitivity to these bottlenecks depends on their swimming capacity

Introduction

When speaking of animal habitats in a landscape perspective, we may be inclined to imagine clearly defined stable patches either isolated or connected by animal movement. In reality, environmental parameters delimiting habitats and determining landscape connectivity are often subject to substantial fluctuations. In dynamic ecosystems, the distribution of habitat patches changes spatially over time ("shifting habitat mosaic", Stanford and others 2005; Wimberly 2006) and so does their accessibility characterised by "transient windows of connectivity" (Zeigler and Fagan 2014). Several spatio-temporal scales may be involved in such dynamics determined by natural or anthropogenic drivers. For instance, distribution of vegetation cover (and thus of habitat patches) in a landscape may be re-set by volcano eruptions or earthquakes occurring on the temporal scales of centuries or thousands of years, or by more frequently recurring disturbances, such as fire or violent storms (Zeigler and Fagan 2014). In river floodplains, large-scale "reshuffling" of habitat mosaic results primarily from major flood events (Hohensinner and others 2011), while natural or artificial fluctuations of environmental parameters (e.g. temperature or water level), occurring on the daily or hourly basis, may affect habitat patch distribution and connectivity at finer spatio-temporal scales (Capra and others 2017; Tonolla and others 2010).

Theoretical modelling has allowed to explore the drivers of metapopulation persistence in dynamic mosaic landscapes (Fahrig 1992; Keymer and others 2000), demonstrating the importance of matching between spatio-temporal scales of landscape dynamics and the life history traits of an organism, such as its life span and dispersal capacity. Animal life cycle may involve movement related to changes of vital space between life stages, most evident in species with complex life cycles shifting between terrestrial and aquatic, or marine and freshwater environments. Furthermore, within the vital space of each life stage, daily or seasonal movements between different habitat types may also occur

(Figure 1). The term “connectivity fractal” has been suggested by Sheaves (2009) to describe the pattern produced by « the hierarchy of migrations at a variety of scales that connect a variety of habitats in complex ways”.

For understanding population dynamics within a landscape, it is crucial to link the habitat-patch-dynamics perspective with a temporal perspective on the organism’s life history including its changing dispersal capacity (Wiens 1976). This involves considering landscape structure and landscape connectivity in terms of propensity or resistance to movement (Baguette and others 2013; Taylor and others 1993). The landscape may thus be seen as an organism- and stage-specific map of habitat patches connected by “highways”, “backroads”, “barriers” etc. Furthermore, as the sequence of life cycle events occurs in a certain non-random and non-reversible order, taking a chronological approach is necessary for understanding “life cycle connectivity” within a given landscape.

Empirical studies of habitat distribution and landscape connectivity are challenging in large dynamic ecosystems, as they require spatio-temporally explicit data acquired at appropriate scales and a sufficiently fine resolution. Where direct observations of movement are difficult, functional connectivity modelling offers a way of quantifying and predicting habitat distribution and accessibility (Adriaensen and others 2003). It became particularly promising in the view of technological developments in remote-sensing and environmental modelling allowing for access to continuous environmental data with high resolution in space and time (Carbonneau and Piégay 2012; Neumann and others 2015). When supported by good knowledge of species ecology and dispersal capacity, these tools allow producing map sequences of habitat patch distribution and landscape permeability for movement.

Habitat accessibility can then be assessed with least-cost modelling, whereby least-cost paths correspond to “effective distances” between habitat patches estimated to have the lowest energetic cost and a maximum potential of survival (Adriaensen and others 2003;

Zeller and others 2012). This approach has allowed identifying terrestrial wildlife corridors in conservation context at the scales from hundreds of kilometers for large mammals (Rouget and others 2006) to few hundreds of meters for amphibians (Ray and others 2002) and invertebrates (Sutcliffe and others 2003). It has also been applied in riverscapes (Foubert and others 2019; Hanke and others 2014) and seascapes (Caldwell and Gergel 2013), but, until recently, hardly used in highly dynamic aquatic systems (but see Foubert and others 2019).

Macrotidal estuaries represent an ecosystem with particularly complex habitat dynamics involving several temporal scales. Daily tidal dynamics interact here with seasonal patterns of freshwater discharge, driving environmental variability (salinity, water level, current velocity and direction) and creating high spatio-temporal habitat heterogeneity. The extremes of such variation can be observed in the intertidal habitats (tidal creeks, salt marshes, mudflats), transformed within hours from nearly terrestrial at low tide to aquatic at high tide. These highly productive habitats are of particular ecological value, as they are an important part of nurseries for many fish and invertebrate species (Bretsch and Allen 2006; Rountree and Able 2007), representing functional habitats, which contribute to their feeding, growth and survival at early stages and offer refuge from predators (Cattrijsse and Hampel 2006; Rountree and Able 2007). Importantly, spatial distribution of optimal nursery habitat patches changes with the progression of the tide due to water level and flow velocity fluctuations creating a true “shifting habitat mosaic” on very short temporal scales. Juveniles of many marine and estuarine fish species have adapted their behaviour to the tidal cycle, effectuating daily migrations to temporarily available habitats (Gibson 2003; Laffaille and others 2001; Martinho and others 2008) or using strong tidal currents (selective tidal transport) to advance on a larger spatial scale in a required direction (Forward and Tankersley 2001).

Many of today's estuaries have been strongly degraded by human activities (Lotze and others 2006). Strategical nodes for navigation and integrators of basin-scale processes, they have a long history of morphological and physico-chemical alteration: channelization, shoreline armoring, as well as upstream-derived impacts such as pollution, changes of river flow regime, or sediment transport. This could have several effects on the habitat dynamics in the estuarine intertidal zones. First, habitat patch availability may be reduced through modification of estuarine morphology either throughout the tidal cycle or at its specific steps. Second, connectivity between available habitat patches might be temporarily disrupted during the tidal cycle, impeding the organisms, which colonise them, to complete their tidal migration cycle.

The objective of our work was to quantify fish habitat availability and accessibility in a macrotidal human-impacted estuary using a chronological map-based modelling approach. We applied tools from functional landscape modelling developed for riverscapes (Roy and Le Pichon 2017) to the case of tidal migration of juvenile European seabass (*Dicentrarchus labrax*) towards summer nurseries of the Seine estuary at the moment of their colonisation. Our study organism is a marine species with a well-documented life-cycle and extensive experimental evidence on swimming capacity at different stages. Specific questions we asked for seabass were: i) How do water level fluctuations affect the extent and distribution of its estuarine nursery habitats? ii) Does a morphologically modified estuary allow for a continuous functional connectivity of the nursery habitats on a large scale and thus for their colonisation by early juveniles?

To address these questions, we considered two temporal scales of variation and conducted both an intra-annual and an intra-tidal analysis. We first tested for the effects of a range of tidal coefficients (TC) and two discharge levels on seabass nursery availability at high tide. Then, for two contrasted cases of hydrological conditions, we quantified nursery

and ebb habitat availability at different steps of the tidal cycle and modelled initial colonisation of these habitats by seabass juveniles. Throughout the paper we used the term "estuarine colonisation" to designate the process of first access of young juveniles from the estuarine mouth to the whole extent of estuarine nurseries up to the upstream limit of their salinity preferences. This large-scale and potentially multi-step advancement profits from selective tidal transport during the flood stages of the tidal cycles. "Estuarine colonisation" results in the establishment of juveniles in certain areas of the estuary, where they were not initially present, and where they can then enter daily cycles of moving between patches of habitat available at different moments of the tide, or "tidal migrations" (Rountree and Able 2007, Sheaves 2009).

Materials and Methods

Study site

The Seine estuary (Figure 2) is an example of a large macrotidal estuary of the European Atlantic coast highly modified by human activities (Tecchio and others 2016). It is characterised by a semidiurnal regime and tidal amplitude of 8.5 m in the mouth area (Lafite and Romaña 2001). The spatial extent of tidal waters covers 170 km of river length, and is limited by the Poses dam upstream. The mean annual Seine river discharge measured at Poses is 450 $m^3 s^{-1}$ (50 to 2200 $m^3 s^{-1}$).

Originally, the mouth of the Seine estuary was a large and shallow braided system characterised by islands, mobile sandbanks, and extensive intertidal areas with mudflats and salt marshes (Avoine and others 1981; Lesourd and others 2016; Figure 2), while the upstream freshwater part was a meandering river with numerous islands, shoals and pools. Since 1834, the Seine estuary has been experiencing morphological and sedimentary

modifications to secure boat traffic and stabilise river flow through channel containment, dredging, diking and island removal. Furthermore, the Normandy Bridge construction (1995), and the new port extension of Le Havre (2006) have considerably modified the structural aspects and the hydrodynamic conditions at the Seine estuary, causing further loss of intertidal habitats. Separating the main channel from the riverbanks by submersible dikes has narrowed the estuary (Grasso and Le Hir 2019) and restricted its lateral connectivity. Altogether, the estuary has lost 78% of its intertidal areas and 80% of the islands since the beginning of the 20th century (Lafite and Romaña 2001; Cuvilliez and others 2009), with 76% of banks in the estuarine mouth being diked (Foussard and others 2010). The nursery capacity of the Seine estuary has been strongly affected by these changes, for instance, for flatfish, it has been estimated to be reduced by 42% (Rochette and others 2010).

Study species

European seabass (*Dicentrarchus labrax*) is a highly exploited fish species of the North East Atlantic (NEA) coast, whose northern stock has been declining over recent years (López and others 2015). The life cycle of NEA populations takes place between marine, coastal and brackish habitats. Seabass spawn offshore in early spring with post-larvae spending about a month in the unstratified waters of the English Channel (Jennings and Pawson 1992). Nursery settlement at the NEA coast occurs between April and September, about 2-3 months upon hatching, followed by the metamorphosis into juveniles between 50 and 110 days post-hatch (Jennings and Pawson 1992; López and others 2015). In spring, once the water temperatures increase, assisted by tidal currents, seabass juveniles colonise coastal and estuarine nurseries and start daily migrations between subtidal and intertidal habitats in poly- and mesohalin zones (Jennings and Pawson 1992; Cabral and Costa 2001). A high local site fidelity has been observed, with juveniles staying for longer periods in proximity of the same nursery areas

196 (Green and others 2012). The tidal migrations continue until the onset of cold temperatures in
197 the fall, when the juveniles move to deeper areas of the estuary or to coastal habitats (Kelley
198 1986). Young seabass spend the first 2-4 years of their life in close association with the
199 estuaries, after which they shift to living in marine and coastal environments (López and
200 others 2015).

201 First-year juveniles of seabass start tidal migrations at the size of 10-15 mm (Jennings
202 and others 1991) and reach about 60 mm at the end of their first summer (Kelley 2002).
203 Dispersal capacity of early stages is rather low (with expected *in situ* swimming speeds of
204 about 0.03-0.13 m s^{-1} for fish under 30 mm; Leis and others 2012). As many marine and
205 catadromous species, juveniles of seabass appear to have the capacity of using selective tidal
206 transport and are guided by environmental cues, such as temperature and low salinity (Pickett
207 and Pawson 1994; López and others 2015). The latter facilitate and orient their movement
208 towards the nurseries located in tidal estuaries and coastal salt marshes or mangroves
209 (Jennings and Pawson 1992). Transport with tidal currents may thus be assumed as the
210 predominant mechanism for estuarine colonisation, but it may be complemented by small-
211 scale movement in shallow areas along the shores or by using back eddies or other slack water
212 to avoid strong currents in the channel (Pickett and Pawson 1994). Furthermore, vertical
213 position selection in the water column presumably facilitating the adjustment of their
214 movement to flow velocity patterns has been reported for seabass larvae and juveniles (López
215 and others 2015). Own swimming capacity of juveniles increases rapidly with growth and
216 reaches about 0.3-0.6 m s^{-1} by the end of the first year. Optimal speeds for late juveniles are
217 predicted at temperatures between 7 and 22°C; Claireaux and others 2006).

218 The highest abundances of seabass juveniles are found in the euhaline and mesohaline
219 zones (Selleslagh and Amara 2008). Shallow (< 2 m deep), turbid and muddy habitats typical
220 of mudflats, salt marshes and tidal creeks have been described as rich feeding grounds

221 particularly prone to becoming seabass nursery habitats (Cabral and Costa 2001; Cattrijsse
222 and others 1994) and recent stable isotope data confirm an important contribition of intertidal
223 zones to their diet (Day & Brind'Amour, unpublished data for the Seine estuary). Field
224 observations indicate that most of the seabass tidal feeding occurs during the flood and the
225 high tide (Laffaille and others 2001). Nearly no quantitative information exists on their
226 behaviour during the ebb and the low tide. During these tidal phases they have been observed
227 to stay in the areas of low flow velocities in proximity to the high-tide nurseries (personal
228 communications E.Feunteun, S.Duhamel), with some individuals remaining in warm tidal
229 pools isolated from the main stream during low tide (Pickett and Pawson 1994; Kelley 1986).
230 In the Seine estuary, this behaviour has also been reported in the intertidal areas behind the
231 dikes (pers. communication E.Feunteun). However, as this behavioural strategy involves
232 substantial risks (desiccation, exposure to predators), we may expect only a very minor
233 fraction of the population to use it.
234

235 ## GIS-based analysis

236 *Water depth and habitat mapping*

237 Based on temperature and discharge time series at the estuarine mouth (Online Resource 1),
238 we identified the period between April 1st and November 15th as the main period of nursery
239 use. This corresponds to the time window following the first spring river floods and when
240 temperature exceeds +10°C (a physiological threshold of feeding activity; Pastoureaud 1991).
241 For the intra-annual comparison of habitat distribution, we used ranking analysis and selected
242 two discharge levels and four tidal coefficients (TC) covering the variability of hydrological
243 conditions occurring during the time window considered: 250 $m^3 s^{-1}$ and 800 $m^3 s^{-1}$ exceeded
244 60% and 5% of time respectively, and TC 45, TC 65, TC 80 and TC 115 exceeded 85%, 60%,
245 35% and 2% of time respectively. Tidal coefficients as high as 115 occurred during extreme

246 spring and fall tides, while variation in tidal coefficients in the summer was well covered by
247 the range between TC 45 and TC 85 (Supplementary Figure S1c).
248 High tide water levels across the estuary were estimated statistically using a model
249 based on the interpolation of tidal heights at eighteen gauges distributed over the estuary
250 between Honfleur and Poses. For the intra-tidal analysis, a 3D-hydrodynamic model of the
251 Seine estuary was used to calculate water level, current velocity and salinity for a
252 hydrologically average year (2010; Supplementary Figure S1b) at a time step of 15 min
253 (MARS-3D; Le Hir and Lafite 2012). We expected habitat surface decrease to be the major
254 driver of fragmentation and connectivity disruption. We thus selected one discharge level
255 (250 $m^3 s^{-1}$) and two tidal coefficients (TC 52 and TC 85) observed in combination in 2010 to
256 cover hydrological conditions resulting in most contrasting patterns of high tide habitat
257 distribution , and achieve the closest possible match to the intra-annual analysis.
258 A regular square grid with each cell covering 5 m x 5 m, was chosen for all GIS-based
259 analyses as a compromise between i) the precision of habitat patch and barrier (e.g.
260 submersible dikes) representation and ii) the calculation time necessary for least-cost
261 modelling. For both intra-annual and intra-tidal analyses, maps of water depths were produced
262 for each discharge level–TC combination and for each considered tidal step based on the
263 difference between the estimated water level and LIDAR-based topo-bathymetric data (GIP
264 Seine Aval) for each cell of the grid.
265 In the following, when referring to the intra-tidal analysis, we use the term “tidal time
266 point” (t_N) to delimit a specific point (“snapshot”) of environmental conditions in time, while
267 “tidal time step” corresponds to the conditions in the interval (t_N-t_{N+1}) between two
268 subsequent tidal time points. Flood thus starts at t_1 (0 min) and ends with t_{14} (195 min), high
269 tide occurs between t_{14} and t_{24} (345 min) and the ebb between t_{24} and t_{49} (720 min)
270 (Supplementary Figure S2). To capture key tidal changes of habitat availability and

connectivity, the flood and the ebb were divided into five time steps each (e.g. t_1-t_5, t_5-t_7 etc.) based on two criteria: the degree of estuarine dike submergence (Figure 2) and the degree of tidal creek inundation along the upstream-downstream gradient (see insets in Figure 3).

The spatial extent considered for this study was determined by the area with the mean salinity above 0.5‰ over the tidal cycle at median TC (70). In the NEA estuaries, the post-larvae have been reported to arrive to coastal areas early in spring and spend at least 30 days in the proximity of the estuaries before colonising them (Jennings and Pawson, 1992). Basing upon expert opinion, we assumed that in spring, early juveniles occupy moderately shallow areas of the mouth of the Seine before entering the tidal cycle to access intertidal nurseries for the first time (personal communication S.Duhamel). The departure habitat for colonisation modelling was thus defined as estuarine mouth areas with 0.2-5 m depth (at low tide) and a minimal patch size of 10 ha (Supplementary Figure S3). Tidal seabass nurseries were defined as shallow areas (0.2-2 m at each time step of the flood) with either sandy or muddy substrate (Fritsch 2005). Their distribution was estimated by intersecting maps of dominant (>50%) bottom substrates in subtidal and intertidal areas (Online Resource 2) with water depth maps. Having limited information on the low tide habitat selection, we chose a simple definition as shallow areas (0.2-2 m) with current velocities not exceeding maximum juvenile swimming capacity tested (< 0.3 m s^{-1}) corresponding functionally to “refuge habitats”. The spatial resolution of our data did not allow us to consider temporary tidal pools as potential refuge habitats.

A value of 100 m^2 was chosen as a minimal patch size, smaller elements being visually identified as geomatic artefacts. For the intra-annual analysis, only high-tide nursery habitats were mapped, while for the intra-tidal analysis, both nursery and refuge habitats were mapped at five time points of the flood (t_5, t_7, t_9, t_{11}, t_{14}) and ebb (t_{27}, t_{30}, t_{34}, t_{39}, t_{45}). To compare habitat distribution along the longitudinal (upstream–downstream) and horizontal

(north-south) axes of the estuary, we distinguished between six sectors: the estuarine mouth, the area with tidal creeks, and the upstream channel located either to the north or to the south of the main channel (see Online Resource 3 for a map).

Resistance mapping

We assumed that key factors driving estuarine permeability for the movement of early seabass juveniles were current velocities in the areas submerged at each tidal time step. Resistance values were assigned to each map pixel based on the current velocities. The current could thus i) be neutral to movement (R=1); ii) facilitate movement (R<1); iii) impede movement (R>1); or iv) be so high as to be avoided by the juveniles and thus considered in the model as an impassable barrier (R=10 000).

As our connectivity model described below necessitates 2D-maps of riverscape resistance to movement, flow velocities from MARS-3D model in subtidal zones were averaged over the water column and across each time step. The choice of taking the average value was a compromise allowing to both not underestimate the transport capacity of the tide and to dampen the potential barrier effects in the most fast-flowing areas potentially avoided by the juveniles through adjustment of their vertical position in the water column. Average flow velocities per grid cell were divided into 6 classes. The mean of each class V_x (0.05, 0.2, 0.5, 0.85, 1.1, > 1.2 m s^{-1}) was used for the calculation of resistance values. In the intertidal areas (mudflats, tidal creeks), mean flow velocities were estimated for each tidal time step based on earlier field measurements (Online Resource 2). Current velocities below 0.05 m s^{-1} were assumed neutral for movement. Velocities between 0.05 and 1.2 m s^{-1} were assumed to facilitate movement, and resistance values R_x were calculated as inversely proportional to 0.05 m s^{-1} (considered equivalent to neutral to movement) ($R_x = V_x / 0.05$). We assumed that flow velocities above 1.2 m s^{-1} (the fourfold of the average juvenile's own speed in their first summer) would be avoided by the juveniles (due to potential risk of mortality or impingement

by the flow) and considered them in the model as barriers (R=10 000). Dikes, unless submerged by at least 0.2 m, were mapped as pixels out of water. Based on these principles, resistance maps were produced for each tidal time step (Figure 3).

Least-cost modelling of habitat connectivity during the tide: a chronological approach

We used ANAQUALAND (Le Pichon and others 2006) and ARCGIS 10.3 to estimate estuarine mouth connectivity to seabass nursery and refuge habitats across the estuary over the tidal cycle. ANAQUALAND requires 2D-raster maps of habitat patches and riverscape resistance to movement as input, and takes into consideration an upstream-downstream (or vice-versa) orientation of the flow direction. The software uses least-cost modelling to calculate minimum functional distance to the nearest habitat patch for each pixel of the map. To distinguish between pixels connected or not connected to a habitat of interest at a given point in time, we applied a swimming-speed-dependent threshold value or "mobility coefficient" (Roy and Le Pichon 2017) which varied depending on the tested scenario (see below). Least-cost modelling of tidal flood phase was carried out for all scenarios. Furthermore, for the lowest swimming speed scenario (see below), several complete tidal cycles were modelled. We used a chronological principle: starting from departure patches at low tide, connectivity between habitat patches was modelled over successive time steps (see Online Resource 4 for details). Only habitat patches connected to the previous step (t_N) of the tidal cycle were taken into account for modelling each subsequent time step (t_{N+1}) (Figure 4). During the high tide (t_{14}-t_{24}), we assumed a multidirectional small-scale exploratory movement between neighbouring nursery patches driven by feeding behaviour rather than further directed colonisation of the estuary in its longitudinal extent.

A sensitivity analysis was conducted to cover several levels of mobility between early spring juveniles with very weak swimming capacities (0.05 m s^{-1}) and summer juveniles of up to 6 cm total length progressively acquiring swimming speed. The expected sustained

346 swimming speed of the juveniles at the end of the first summer was calculated as a fivefold of
347 their body length per second (0.6*5= 0.3 m s^{-1}; Leis and others 2012) and was in line with the
348 ranges of optimal speeds reported for late juveniles (Claireaux and others 2006). We modelled
349 four scenarios corresponding to four swimming speeds (0.05; 0.1; 0.2; 0.3 m s^{-1}). The
350 colonisation front for each scenario was determined as the position of the most-upstream
351 nursery habitats accessible at the beginning of the high tide.

352 To estimate the duration of complete colonisation of the estuary by early juveniles, we
353 modelled successive tidal cycles including ebb and low tide phases for the 0.05 m s^{-1} scenario
354 (at both TC 52 and TC 85), until the upstream limit of the study area was reached. Starting
355 from the second tidal cycle, the refuge habitat patches accessible at the end of the previous
356 tidal cycle were used as the departure habitat of the following tide. The low tide could
357 potentially be used for further advancing the colonisation front, if the individuals restarted
358 directed movement in the upstream direction already at this tidal stage. However: i) the actual
359 behaviour of the juveniles at low tide is largely unknown; ii) the current velocities at this tidal
360 phase are very low and multidirectional; iii) the own swimming speed of the juveniles tested
361 in this scenario was very low (0.05 m s^{-1}) and would allow them to advance in areas with no
362 assisting flow at most by 450 m over the low tide duration (2.5 h). Considering these
363 uncertainties, we chose not to take potential low-tide movement into account, and assumed in
364 the model, that the position of the juveniles in the beginning of the next flood would be
365 approximately the same as in the end of the preceding ebb.
366
367

Results

Intra-annual analysis: potential nursery availability at high tide

Our comparison of high-tide habitat distribution across different hydrological conditions showed two main trends: i) a non-linear response of potential nursery surfaces to tidal coefficient gradient on both north and south sides (Figure 5a), and ii) consistent differences in habitat distribution between estuarine sectors (Figure 5b). The total area of potential estuarine nursery surface at high tide varied by about 80 ha across the hydrological conditions tested. The extremes of potential nursery surface were found at the higher discharge level (800 $m^3 s^{-1}$) with the minimum of 351.3 ha at TC 115 (the highest TC tested) and the maximum of 434.4 ha at TC 45 (the lowest TC tested).

Under all hydrological conditions, potential habitats were predominantly located in the estuarine mouth area (52-70% on the north side, and 54-87% in the south) with the rest distributed between the tidal creek sector and the intertidal zones along the channel (Figure 5b). Potential habitat availability in different sectors on the north side was rather stable across different hydrological conditions: it varied moderately in the mouth area, and, at both discharge levels, showed a progressive increase in tidal creeks and a decrease in the intertidal zones along the channel with augmenting TC (Figure 5b). On the south side, the relative distribution of high-tide nurseries between the mouth area and other sectors was less balanced in space and time. For instance, the surface of potential nursery habitats in the mouth area decreased by over 100 ha between the lowest and the highest TC (Figure 5b). Nursery availability in other sectors was considerably lower on the south side compared to the north side. Only in tidal creeks did it increase along the tested TC gradient with nursery surface multiplied by four between the lowest and the highest TC at both discharge levels (Figure 5b).

Intra-tidal analysis: dynamics of potential nursery availability

We found an even higher level of variation in potential nursery availability when zooming into the dynamics of a single tidal cycle. During the tide, the distribution of potential nursery habitats progressively shifted in the lateral and longitudinal direction resulting in no overlap between the low-tide and the high-tide habitat patches (Figure 6). In the beginning of the flow, most habitat patches were located in the downstream areas of the subtidal zone. With the tidal water level rise, intertidal zones became progressively submerged and hydrologically reconnected to the main channel, whereas some nursery patches in the mouth area became unfavorable. This resulted in an unbalanced distribution of low-tide versus high-tide habitats at the estuarine scale with high-tide “desert areas” (stretches completely lacking habitat) emerging along the diked channel both on the south (downstream part) and the north (first loop of the Seine) side (Figure 6).

The intra-tidal decrease of the habitat surface in the mouth area was particularly pronounced in the south: habitat surface available there was four to nine times lower (at TC 52 and TC 85 respectively) at high tide compared to low tide (Figure 7b). This decrease was moderate in the north, where low-to-high-tide relation of habitat surface was 2:1 at both TCs. Temporary loss of habitat in the mouth area was compensated by a substantial increase of habitat surface in the tidal creek area (1:4 at TC 52 and 1:8 at TC 85) in the north, but not in the south, where very little intertidal habitat was available throughout the tidal cycle at both tidal coefficients (Figure 7b).

Tidal coefficient also affected the lateral habitat distribution and degree of fragmentation. At TC 52, the lateral extent of habitats was smaller and the strips of habitat patches along the diked channel upstream were more continuous, whereas, at TC 85, many of

these patches became very narrow or completely unavailable due to a drastic water depth increase in this area (insets in Figure 6).

Connectivity analysis: nursery accessibility from the estuarine mouth

Both tidal coefficients and fish swimming speeds tested had a strong effect on the colonisation front reached within a single flood (Figure 8). Advancement in the estuary was faster at the lower tidal coefficient (TC 52). With a minimal own speed of 0.05 m s^{-1}, using the upstream-directed current, the juveniles would reach the areas above the largest tidal creek on the north side within a single tide (Figure 8a). Increasing swimming capacity advanced their colonisation front progressively on both the north and the south side, with an average gain of 9.4 km (along the shoreline) with every 0.1 m s^{-1} of own speed added. The swimming speed of 0.3 m s^{-1} resulted sufficient for colonising the whole estuary within a single flood.

At the higher tidal coefficient (TC 85), not only did the colonisation front advance substantially slower compared to TC 52 in each of the swimming speed scenarios, but also the extent of this difference varied depending on the side of the estuary. Thus, while on the north side, the colonisation front of the 0.05 m s^{-1} was situated 3.4 km further downstream compared to the same scenario at TC 52, on the south side, this gap was about three times larger (Figure 8). It is only for the swimming speed of 0.2 m s^{-1}, that colonisation fronts at TC 85 became approximately aligned between the north and the south side (Figure 8b). Finally, at TC 85, the full extent of the estuary could not be colonised within a single tidal cycle in the 0.3 m s^{-1} scenario: 1.8 km and 3.7 km remained until the upstream limit of the study area on the north and south side respectively.

Importantly, while increasing juvenile swimming speed accelerated upstream advancement of the colonisation front, the effective gain in total accessible habitat surface was very moderate. The number of habitat patches reached at high tide was multiplied by two

(TC 52) and four (TC 85) between the lowest and the highest swimming speed scenarios, but this corresponded to only 30 % increase of the total habitat surface accessible across the estuary (Supplementary Figure S4). This result was consistent with the general pattern of habitat fragmentation along the estuary with large habitat patches available in the mouth area and a high number of smaller habitat patches present in the upstream areas (Figure 6).

A facilitating effect of the lower tidal coefficient on the estuarine colonisation became particularly evident when modelling progressive colonisation of the estuary at the lowest swimming speed (0.05 m s^{-1}). The full colonisation of the estuary necessitated five tidal cycles at TC 52 and seven cycles at TC 85. Even if at both TCs the mouth areas of some of the largest tidal creeks were reached rapidly, a second tidal cycle appeared necessary for full colonisation of the lateral dimension (inset in Figure 9). As mentioned above, this result did not take into account that some further advancement in the creek could have eventually been made during the high tide of the first tidal.

Successive tidal cycle modelling revealed the emergence of temporal connectivity bottlenecks for weak dispersers. In particular, local connectivity disruptions behind the colonisation front were observed at some stages of the flood in the first loop of the Seine (Supplementary Figure S5). Fish that would have advanced above this area in the beginning of the flood would remain in an area disconnected from downstream habitat patches at later stages of the flood.

Discussion

The term “moving target“ has been coined in conservation biology to underline the importance of considering habitat patch dynamics tracked by animal movement for establishing meaningful measures of protection (Bull and others 2013). Highly dynamic environments represent a challenge for understanding and quantifying patterns of habitat

availability, especially, because not only the structure (patch size and distribution), but also functional connectivity of such landscapes varies in space and time (Zeigler and Fagan 2014). Characterised by pronounced spatial dynamics of habitat turnover and connectivity at several temporal scales, macrotidal estuaries are perfect examples of environments with constantly "moving targets".

Previous studies have mapped large-scale nursery availability (Nagelkerken and others 2015; Whaley and others 2007), and emphasised the paramount importance of the intra-habitat connectivity for the value of estuarine and coastal nurseries (Secor and Rooker 2005; Sheaves and others 2015). However, few have looked into the intra-tidal dynamics of the estuarine habitat availability. Trapping and video observations during flood and ebb tides recorded the transient habitat utilization by young stages of many necton species (Bretsch and Allen 2006; Ellis and Bell 2008; Laffaille and others 2001). However, technically challenging, such field studies are limited in spatial scale and temporal resolution. Spatio-temporally explicit approaches, which integrate hydrological and biotic connectivity of a landscape, appear indispensable for quantifying habitat dynamics and accessibility in large estuaries. Our study represents, to our knowledge, the first case of least-cost modelling application to estuarine habitats and the first example of investigating intra-tidal habitat dynamics across a large estuary with such a fine spatio-temporal resolution.

Spatio-temporal bottlenecks in estuarine habitat availability and connectivity

In the pristine Seine estuary (large, shallow, and with weak lateral slopes), water level increase during the tidal cycle must have led to a continuous shifting of shallow areas from mudflats in the mouth area into tidal creeks and salt marshes (lateral shifts) as well as in the upstream direction (longitudinal shifts). In these conditions, seabass juveniles probably had access to nurseries throughout the tidal cycle and at any hydrological conditions. We observe

no spatio-temporally continuous access to shallow-water nurseries across the Seine estuary in its current highly modified state. Altogether, we find a highly counter-intuitive result: the relationship between water level and potential nursery surface availability is inversed. Thus, in contrast to what we would expect in a pristine system, in the modern Seine estuary, advancing tidal flow results in a dramatic drop of the total nursery habitat surface. This is particularly pronounced on its south side, where temporary gaps in nursery distribution emerge.

Highly modified topography of the Seine estuary is the most likely explanation for this "surprise", and this conclusion is in line with previous studies of artificialised floodplains of the upstream Seine river (Le Pichon and others 2009) and the Saint-Lawrence River (Foubert and others 2019). Harbour expansion, channel dredging, and creation of steep banks along submersible dikes led to a massive loss of the intertidal zones (Cuvilliez and others 2009), and introduced artificial « breaks » in the cross-sectional profile of the estuary (Supplementary Figure S6). Consequently, in many areas of the mouth zone, no gradual transition between the subtidal and the intertidal zones exists anymore. Instead, with the rising water level, shallow patches get fragmented and small, and, at some point, disappear locally until a critical water level allowing for dike submersion is reached, and the intertidal zones behind them become available for colonisation. Dike construction and channel dredging have also modified the estuarine permeability to movement. Our results show that flow velocities along the dikes increase substantially during the tide. At some stages of the tide, channel current velocities are so high that juvenile movement may only be possible in remaining narrow strips of slow flow velocity along the channel margins.

The role of dispersal capacity for estuarine colonisation

In order to predict an organism's propagation through a landscape, we need to consider its dispersal capacity and behaviour in interaction with the environment it encounters. In a riverscape, the extent of fish movement is predominantly determined by the animal's swimming capacity, the flow velocities, and the direction of the current. Behavioural strategies of marine and estuarine fish, such as selective tidal transport, allow them to augment movement range and reduce related energy costs in systems exposed to tides and current reversal (Forward and Tankersley 2001). Here, testing several scenarios allowed us to analyse the effects of swimming speed on the estuarine colonisation using selective tidal transport. We show that, early juveniles with a low swimming capacity need several successive tides to reach high-tide nurseries in the entire study area, while a single tide would be sufficient by the end of their first summer.

Our results, representative of hydrological conditions at medium discharge ($250 m^3.s^{-1}$), suggest that colonisation is facilitated by low rather than by high TCs. On the occasion of spring flooding, extreme river discharge levels (potential triggers of estuarine colonisation; Jennings and Pawson 1992) may occur in the Seine estuary, whereby tidal flood current velocities are counteracted by the river discharge (unpublished simulations of MARS-3D model, Lemoine). This effect, which we, unfortunately, could not explore in the framework of this study, should probably reduce both the speed of juvenile advancement in the estuary and the extent of estuarine areas with high currents and thus the potential risk of being swept away at high TCs.

Altogether, our comparison across different steps of the tidal cycle allows for several conclusions. We show that transient local bottlenecks of nursery availability and accessibility emerge in the Seine estuary during specific time windows of the tidal cycle. Our second conclusion is that these bottlenecks are driven both by progressive habitat fragmentation and by locally increasing riverscape resistance to movement. Finally, own mobility of juveniles

appears to play a key role for successful colonisation with weak dispersers obliged to follow a stepping-stone-type colonisation.

Caveats and limitations of least-cost analysis

Chronological modelling approach, proposed here for dynamic environments, requires a careful consideration of the choice of appropriate spatio-temporal scales. The latter should cover the range of variation in both habitat availability and connectivity relevant for the movement of the species with its specific ecological, behavioural and dispersal-related traits. In the case of the seabass juvenile estuarine colonisation, the spatial component had to include both an extent sufficient for covering the entire area of the estuarine mouth containing tidal habitats, and a resolution allowing us to consider narrow tidal creeks and channel banks with high-tide nurseries. Furthermore, the selection of time steps had to capture the structural connectivity changes during the tidal cycle. Remote sensing data and a 2D-hydrodynamic model available for the Seine estuary at high spatio-temporal resolution permitted us to fulfill these criteria.

While our approach provides a highly flexible and spatially relevant framework, some limitations related to biological assumptions and their translation into habitat and connectivity modelling exist. Thus modelled nursery habitat was primarily defined by a combination of water depth ranges and sediment characteristics established based on rare reported field observations of juvenile seabass in the intertidal zones of NEA coast. Ideally, fine-scale field investigations of nursery habitat characteristics, potentially taking into account further dynamic variables (e.g. turbidity, temperature, dissolved oxygen or food availability) would allow for a better delimitation of nursery habitats. Furthermore, in the connectivity analysis applied we could not consider differences in habitat quality and patch size, which could affect patch carrying capacity and juvenile preferences (Teichert and others 2018).

Parametrization of the least-cost analysis itself may also strongly affect its results. Resistance values attributed to each pixel of a riverscape map are a crucial element linking GIS-based data to the organism mobility and dispersal behaviour (Adriaensen and others 2003). Field or mesocosm studies quantifying the effect of high current velocities on early juvenile fish could improve the calibration of riverscape resistance to movement and the precision of the current velocity threshold above which water flow may become a barrier. Further sensitivity analysis may allow for quantification of the effects of these parameters and the related error margins (Beier and others 2008). However, in the case of complex chronological calculations as the ones presented here, investigating ranges of values is rapidly translated into long computation times and a compromise needs to be found. Here we chose to focus on testing a plausible range of juvenile seabass mobility parameters.

Implications for management and conservation

Fish stocks of many marine and estuarine species experience a drastic decline (Christensen and others 2014; Vasilakopoulos and others 2014). Increasing attention has been given in the last decades to identifying population bottlenecks, notably at the sensitive stages of spawning, juvenile colonisation of nurseries and growth, to be targeted by management and conservation efforts (Sheaves and others 2015). In macrotidal estuaries, the nature and drivers of such bottlenecks may be difficult to identify and common-sense assumptions (as simple as “higher water level means more available intertidal habitat”) may prove to be misleading in human-modified systems.

Chronological functional connectivity modelling offers a road for addressing this challenge. Zooming into the processes occurring during tidal cycles helps disentangle the effects of habitat fragmentation and riverscape connectivity and identify the timing of occurrence and location of the transient bottlenecks that may affect habitat colonisation by

juveniles. Maps produced by our approach may be directly used to test and visualize the consequences of different management scenarios, and subsequently guide decision-making (e.g. prioritisation of areas for dike removal or for conservation).

Our work demonstrates that focusing exclusively on the protection and restoration of high tide nurseries may prove inefficient, as they may be disconnected from the succession of habitat patches needed over the tidal cycle. This is an empirical illustration to the notions of "moving targets" (Bull and others 2013), "seascape nurseries" (mosaics of functionally connected habitat patches; Nagelkerken and others 2015) and "transient windows for connectivity" (Zeigler and Fagan 2014) formulated in conservation biology and emphasising the importance of taking the mobile nature of connectivity and habitats into account when planning conservation measures. We suggest that chronological functional connectivity modelling is a valuable tool applicable to any ecosystem where organisms have to cope with highly dynamic environments over their life cycle.

Acknowledgments

This study has been carried out in the framework of the ANACONDHA project funded by the scientific research program of the GIP Seine-Aval. We cordially thank Nicolas Bacq for his invaluable support, ideas and work orientations throughout the project, Sylvain Duhamel, Eric Feunteun, Ronan Le Goff, Mike Pawson, Hélène de Pontual, Florian Rozanska and Stéphanie Moussard for sharing their expertise and time during fruitful discussions at different stages of this project, Jean-Philippe Lemoine for producing MARS-3D model outputs, Eric L'Ebrellec for preparing habitat and water depth maps and providing supplementary data on the Seine estuary, Sylvain Descloux for his support with improving ANAQUALAND, and Amandine Zahm for running part of the tested scenarios. We kindly thank two anonymous reviewers and

609 the editors for their very constructive and insightful comments that helped to substantially
610 improve the manuscript throughout the revision process.

611 **References**

612 Adriaensen F, Chardon JP, De Blust G, Swinnen E, Villalba S, Gulinck H, Matthysen E. 2003.
613 The application of 'least-cost' modelling as a functional landscape model. Landsc Urb
614 Plan 64:233-247.

615 Avoine J, Allen GP, Nichols M, Salomon JC, Larsonneur C. 1981. Suspended-sediment
616 transport in the Seine estuary, France: Effect of man-made modifications on estuary—
617 shelf sedimentology. Mar Geol 40:119-137.

618 Baguette M, Blanchet S, Legrand D, Stevens VM, Turlure C. 2013. Individual dispersal,
619 landscape connectivity and ecological networks. Biol Rev 88:310-326.

620 Beier P, Majka DR, Spencer WD. 2008. Forks in the road: choices in procedures for designing
621 wildland linkages. Conserv Biol 22:836-851.

622 Bretsch K, Allen DM. 2006. Tidal migrations of nekton in salt marsh intertidal creeks.
623 Estuaries Coast 29:474-486.

624 Bull JW, Suttle KB, Singh NJ, Milner-Gulland E. 2013. Conservation when nothing stands
625 still: moving targets and biodiversity offsets. Front Ecol Environ 11:203-210.

626 Cabral H, Costa MJ. 2001. Abundance, feeding ecology and growth of 0-group sea bass,
627 *Dicentrarchus labrax*, within the nursery areas of the Tagus estuary. J Mar Biol Assoc
628 UK 81: 679-682.

629 Caldwell I, Gergel S. 2013. Thresholds in seascape connectivity: influence of mobility,
630 habitat distribution, and current strength on fish movement. Landsc Ecol 28:1937-1948.

631 Capra H, Plichard L, Bergé J, Pella H, Ovidio M, McNeil E, Lamouroux N. 2017. Fish habitat
632 selection in a large hydropeaking river: Strong individual and temporal variations
633 revealed by telemetry. Sci Tot Environ 578:109-120.

634 Carbonneau P, Piégay H. 2012. Fluvial remote sensing for science and management. John
635 Wiley & Sons.

636 Cattrijsse A, Makwaia ES, Dankwa HR, Hamerlynck O, Hemminga MA. 1994. Nekton
637 communities of an intertidal creek of a European estuarine brackish marsh. Mar Ecol
638 Progr Ser 109: 195-208.
639 Cattrijsse A, Hampel H. 2006. European intertidal marshes: a review of their habitat
640 functioning and value for aquatic organisms. Mar Ecol Prog Ser 324: 293-307.
641 Christensen V, Coll M, Piroddi C, Steenbeek J, Buszowski J, Pauly D. 2014. A century of
642 fish biomass decline in the ocean. Mar Ecol Prog Ser 512: 155-166.
643 Claireaux G, Couturier C, Groison A-L. 2006. Effect of temperature on maximum swimming
644 speed and cost of transport in juvenile European sea bass (*Dicentrarchus labrax*). J Exp
645 Biol 209:3420-3428.
646 Cuvilliez A, Deloffre J, Lafite R, Bessineton C. 2009. Morphological responses of an
647 estuarine intertidal mudflat to constructions since 1978 to 2005: The Seine estuary
648 (France). Geomorphology 104:165-174.
649 Ellis WL, Bell SS. 2008. Tidal influence on a fringing mangrove intertidal fish community as
650 observed by in situ video recording: implications for studies of tidally migrating nekton.
651 Mar Ecol Prog Ser 370:207-219.
652 Fahrig L. 1992. Relative importance of spatial and temporal scales in a patchy environment.
653 Theor Popul Biol 41:300-314.
654 Forward RB, Tankersley RA. 2001. Selective tidal-stream transport of marine animals.
655 Oceanogr Mar Biol 39:305-353.
656 Foubert A, Le Pichon C, Mingelbier M, Farrell JM, Morin J, Lecomte F. 2019. Modeling the
657 effective spawning and nursery habitats of northern pike within a large spatiotemporally
658 variable river landscape (St. Lawrence River, Canada). Limnol Oceanogr 64:803-819.

659 Foussard V, Cuvilliez A, Fajon P, Fisson C, Lesueur P, Macur O. 2010. Evolution
660 morphologique d'un estuaire anthropisé de 1800 à nos jours. Fascicule Seine-Aval 2.3.
661 https://www.seine-aval.fr/publication/fasc-evolution-morphologique/
662 Fritsch M. 2005. Traits biologiques et exploitation du bar commun *Dicentrarchus labrax* (L.)
663 dans les pêcheries françaises de la manche et du golfe de Gascogne. Doctoral
664 dissertation, University of Western Brittany.
665 Gibson RN. 2003. Go with the flow: tidal migration in marine animals. Hydrobiologia
666 503:153-161.
667 Grasso F, Le Hir P. 2019. Influence of morphological changes on suspended sediment
668 dynamics in a macrotidal estuary: diachronic analysis in the Seine Estuary (France)
669 from 1960 to 2010. Ocean Dyn 69:83-100.
670 Green BC, Smith DJ, Grey J, Underwood GJ. 2012. High site fidelity and low site
671 connectivity in temperate salt marsh fish populations: a stable isotope approach.
672 Oecologia 168:245-255.
673 Hanke MH, Lambert JD, Smith KJ. 2014 Utilization of a multicriteria least-cost path model
674 in an aquatic environment. Int J Geogr Inf Sci 28:1642-1657.
675 Hohensinner S, Jungwirth M, Muhar S, Schmutz S. 2011. Spatio-temporal habitat dynamics
676 in a changing Danube River landscape 1812-2006. Riv Res Appl 27:939-955.
677 Jennings S, Lancaster JE, Ryland JS, Shackley SE. 1991. The age structure and growth
678 dynamics of young-of-the-year bass, *Dicentrarchus labrax*, populations. J Mar Biol
679 Assoc UK 71:799-810.
680 Jennings S, Pawson M. 1992. The origin and recruitment of bass, *Dicentrarchus labrax*,
681 larvae to nursery areas. J Mar Biol Assoc UK 72:199-212.
682 Kelley D. 1986. Bass nurseries on the west coast of the UK. J Mar Biol Assoc UK 66: 439-
683 464.

684 Kelley D. 2002. Abundance, growth and first-winter survival of young bass in nurseries of
685 south-west England. J Mar Biol Assoc UK 82:307-19.
686 Keymer JE, Marquet PA, Velasco-Hernández JX, Levin SA. 2000. Extinction thresholds and
687 metapopulation persistence in dynamic landscapes. Am Nat 156:478-494.
688 Laffaille P, Lefeuvre J-C, Schricke M-T, Feunteun E. 2001. Feeding ecology of o-group sea
689 bass, *Dicentrarchus labrax*, in salt marshes of Mont Saint Michel Bay (France).
690 Estuaries 24:116-125.
691 Lafite R, Romaña L-A. 2001. A man-altered macrotidal estuary: the Seine estuary (France):
692 introduction to the special issue. Estuaries Coast 24:939-939.
693 Le Hir P, Lafite R. 2012. Projet MODEL: Modélisation validée de l'hydro-morpho-
694 sédimentologie, base physique d'une modélisation environnementale de l'estuaire de la
695 Seine. GIP Seine Aval https://www.seine-aval.fr/projet/model/
696 Le Pichon C, Gorges G, Baudry J, Goreaud F, Boët P. 2009. Spatial metrics and methods for
697 riverscapes: quantifying variability in riverine fish habitat patterns. Environmetrics
698 20:512-526.
699 Le Pichon C, Gorges G, Faure T, Boussard H. 2006. Anaqualand 2.0: freeware of distances
700 calculations with frictions on a corridor. 2.0 edn. Cemagref, Antony
701 https://www6.rennes.inra.fr/sad/Outils-Produits/Outils-informatiques/Anaqualand.
702 Leis JM, Balma P, Ricoux R, Galzin R. 2012. Ontogeny of swimming ability in the European
703 sea bass, *Dicentrarchus labrax* (L.)(Teleostei: Moronidae) Mar Biol Re. 8:265-72.
704 Lesourd S, Lesueur P, Fisson C, Dauvin J-C. 2016. Sediment evolution in the mouth of the
705 Seine estuary (France): A long-term monitoring during the last 150 years. CR Geosci
706 348:442-450.

López R, de Pontual H, Bertignac M, Mahévas S. 2015. What can exploratory modelling tell us about the ecobiology of European sea bass (*Dicentrarchus labrax*): a comprehensive overview. Aquat Living Resour 28:61-79.

Lotze HK, Lenihan HS, Bourque BJ, Bradbury RH, Cooke RG, Kay MC, Kidwell SM, Kirby, MX, Peterson CH, Jackson JBC. 2006. Depletion, degradation, and recovery potential of estuaries and coastal seas. Science, 312:1806-1809.

Martinho F, Leitão R, Neto JM, Cabral H, Lagardère F, Pardal MA. 2008. Estuarine colonization, population structure and nursery functioning for 0-group sea bass (*Dicentrarchus labrax*), flounder (*Platichthys flesus*) and sole (*Solea solea*) in a mesotidal temperate estuary. J App Ichthyol 24:229-237.

Nagelkerken I, Sheaves M, Baker R, Connolly RM. 2015. The seascape nursery: a novel spatial approach to identify and manage nurseries for coastal marine fauna. Fish Fish 16:362-371.

Neumann W, Martinuzzi S, Estes AB, Pidgeon AM, Dettki H, Ericsson G, Radeloff VC. 2015. Opportunities for the application of advanced remotely-sensed data in ecological studies of terrestrial animal movement. Mov Ecol 3:8.

Pastoureaud A. 1991. Influence of starvation at low temperatures on utilization of energy reserves, appetite recovery and growth character in sea bass, *Dicentrarchus labrax*. Aquac 99:167-178.

Pickett GD, Pawson MG. 1994. Sea bass. Biology, exploitation and conservation. Chapman & Hall.

Ray N, Lehmann A, Joly P. 2002. Modeling spatial distribution of amphibian populations: a GIS approach based on habitat matrix permeability. Biodivers Conserv 11**:**2143-2165.

730 Rochette S, Rivot E, Morin J, Mackinson S, Riou P, Le Pape O. 2010. Effect of nursery habitat
731 degradation on flatfish population: Application to *Solea solea* in the Eastern Channel
732 (Western Europe). J Sea Res 64:34-44.
733 Rouget M, Cowling RM, Lombard AT, Knight AT, Kerley GIH. 2006. Designing large-scale
734 conservation corridors for pattern and process. Conserv Biol 20:549-561.
735 Rountree RA, Able KW. 2007. Spatial and temporal habitat use patterns for salt marsh nekton:
736 implications for ecological functions. Aquat Ecol 41:25-45.
737 Roy ML, Le Pichon C. 2017. Modelling functional fish habitat connectivity in rivers: A case
738 study for prioritizing restoration actions targeting brown trout. Aquat Conserv 27:927-
739 937.
740 Schlosser IJ. 1995. Critical landscape attributes that influence fish population dynamics in
741 headwater streams. Hydrobiologia 303:71-81.
742 Secor H, Rooker JR. 2005. Connectivity in the life histories of fishes that use estuaries. Estuar
743 Coast Shelf Sci 64:1-3.
744 Selleslagh J, Amara R. 2008. Environmental factors structuring fish composition and
745 assemblages in a small macrotidal estuary (eastern English Channel). Estuar Coast Shelf
746 Sci 79:507-517.
747 Sheaves M. 2009. Consequences of ecological connectivity: the coastal ecosystem mosaic.
748 Mat Ecol Prog Ser 391:107-115.
749 Sheaves M, Baker R, Nagelkerken I, Connolly RM. 2015. True value of estuarine and coastal
750 nurseries for fish: incorporating complexity and dynamics. Estuaries Coast 38:401-414.
751 Stanford JA, Lorang MS, Hauer FR. 2005. The shifting habitat mosaic of river ecosystems.
752 SIL Proc 29:123-136;

753 Sutcliffe OL, Bakkestuen V, Fry G, Stabbetorp OE. 2003. Modelling the benefits of farmland
754 restoration: methodology and application to butterfly movement. Landsc Urban Plan
755 63:15-31.
756 Taylor PD, Fahrig L, Henein K, Merriam G. 1993. Connectivity is a vital element of landscape
757 structure. Oikos 68:571-573.
758 Tecchio S, Chaalali A, Raoux A, Tous Rius A, Lequesne J, Girardin V, Lassalle G, Cachera
759 M, Riou P, Lobry J, Dauvin J-C, Niquil N. 2016. Evaluating ecosystem-level
760 anthropogenic impacts in a stressed transitional environment: The case of the Seine
761 estuary. Ecol Indic 61:833-845.
762 Teichert N, Carassou L, Sahraoui Y, Lobry J, Lepage M. 2018. Influence of intertidal
763 seascape on the functional structure of fish assemblages: Implications for habitat
764 conservation in estuarine ecosystems. Aquat Conserv 28:798-809.
765 Tonolla D, Acuña V, Uehlinger U, Frank T, Tockner K. 2010. Thermal heterogeneity in river
766 floodplains. Ecosyst 13:727-740.
767 Vasilakopoulos P., Maravelias CD, Tserpes G. 2014. The alarming decline of Mediterranean
768 fish stocks. Curr Biol, 24: 1643-1648.
769 Whaley SD, Burd Jr JJ, Robertson BA. 2007. Using estuarine landscape structure to model
770 distribution patterns in nekton communities and in juveniles of fishery species. Mar
771 Ecol Progr Ser 330:83-99.
772 Wiens JA. 1976. Population responses to patchy environments. Ann Rev Ecol Syst 7:81-120.
773 Wimberly MC. 2006. Species dynamics in disturbed landscapes: when does a shifting habitat
774 mosaic enhance connectivity? Landsc Ecol 21: 35-46.
775 Zeigler SL, Fagan WF. 2014. Transient windows for connectivity in a changing world. Mov
776 Ecol 2:1.

777 Zeller KA, McGarigal K, Whiteley AR. 2012. Estimating landscape resistance to movement:
778 a review. Landsc Ecol 27:777-797.

Figure captions

Figure 1: A life cycle example (inspired by Schlosser 1995) with (a) living space (all habitats) occupied by each stage; (b) example of directed daily movements (e.g. tidal dynamics) of a single stage between habitats; (c) seasonal dynamics of habitat use of another life stage (adult). t_N...t_{N+i} represent points in time, whereby time scales may vary.

Figure 2: The spatial extent of the Seine estuary considered in this study. High-tide wetted area at TC 85 (at 250 m^3 s^{-1}) is presented for 2010. Historical estuarine data is based on the maps of Magin and Magin (1750).

Figure 3: Time-step-specific resistance maps used for modelling upstream movement of juveniles with the flood (two TCs and discharge of 250 m^3 s^{-1}). Colours represent resistance values (R) calculated based on mean current velocities (V).

Figure 4: The principle of habitat patch connectivity calculation between tidal time steps. $H(t_N)$ represents departure habitat at time point t_N; $H(t_{N+1})$ represent patches of potentially available habitat at the next time point t_{N+1}. The dotted lines delineate the areas within threshold functional distances calculated with the least-cost modelling for four hypothetical scenarios. In scenario 4, only the part of $H(t_{N+1})$ in light grey is connected to $H(t_N)$ and retained for the next step of the analysis.

Figure 5: Intra-annual analysis: high-tide nursery surface areas at four TCs and two levels of discharge on the north and south side: a) total potential nursery area; b) potential nursery area by estuarine sector.

804 **Figure 6**: Distribution of nursery habitats in the beginning and at the end of the flood at two
805 TCs and discharge of 250 $m^3 s^{-1}$.
806
807 **Figure 7**: Nursery surface change during the flood at two TCs and discharge of 250 $m^3 s^{-1}$: a)
808 total potential nursery area; b) potential nursery area by estuarine sector.
809
810 **Figure 8:** Colonisation front under different swimming speed scenarios at two TCs and
811 discharge of 250 $m^3 s^{-1}$. Separate arrows are shown for the south and the north, when
812 colonisation fronts on the two sides are not aligned.
813
814 **Figure 9:** Successive tidal colonisation fronts modelled at two TCs and discharge of 250 $m^3 s^{-1}$
815 for the 0.05 m s^{-1} swimming speed scenario. The inset (b) shows details of the lateral
816 intertidal zones colonised at TC 52 with the first tide. Separate arrows are shown for the south
817 and the north, when colonisation fronts on the two sides are not aligned.

Figures

Figure 1

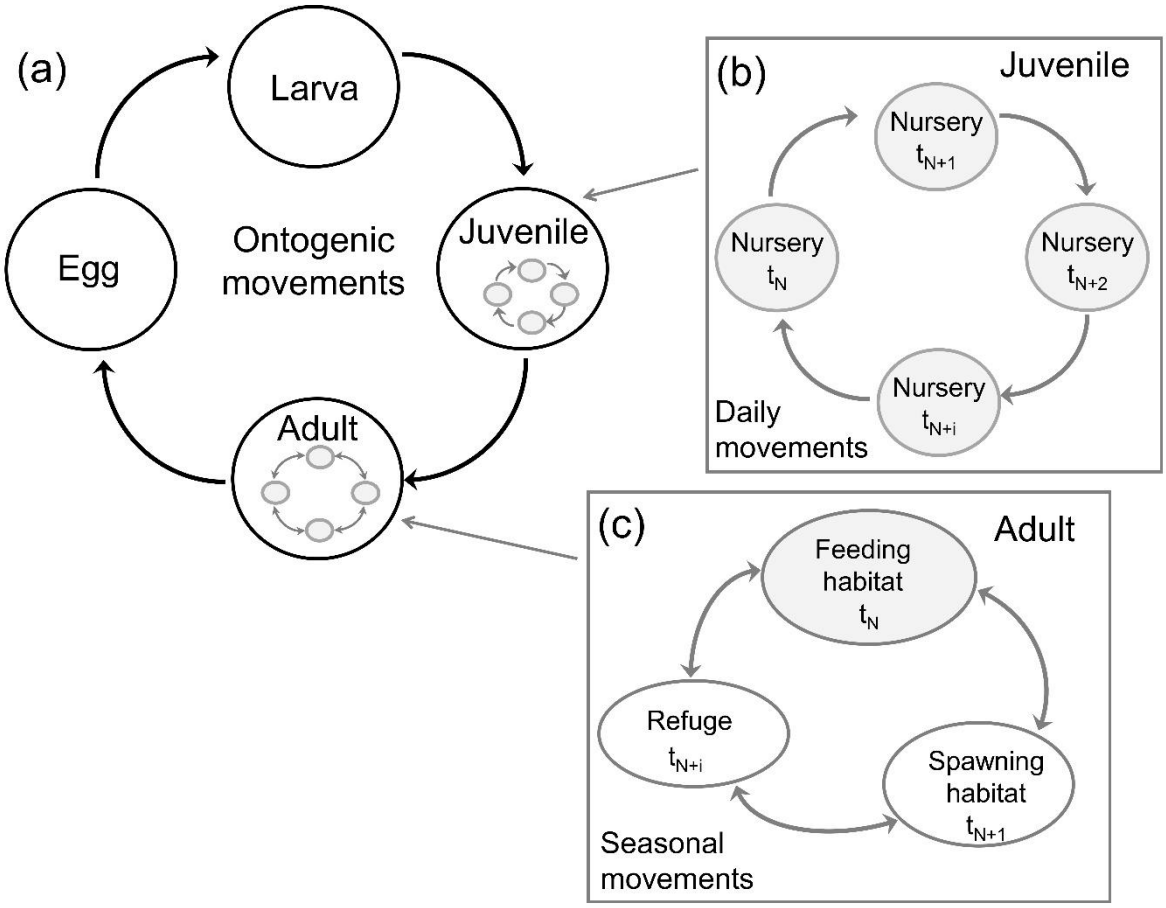

824 **Figure 2**

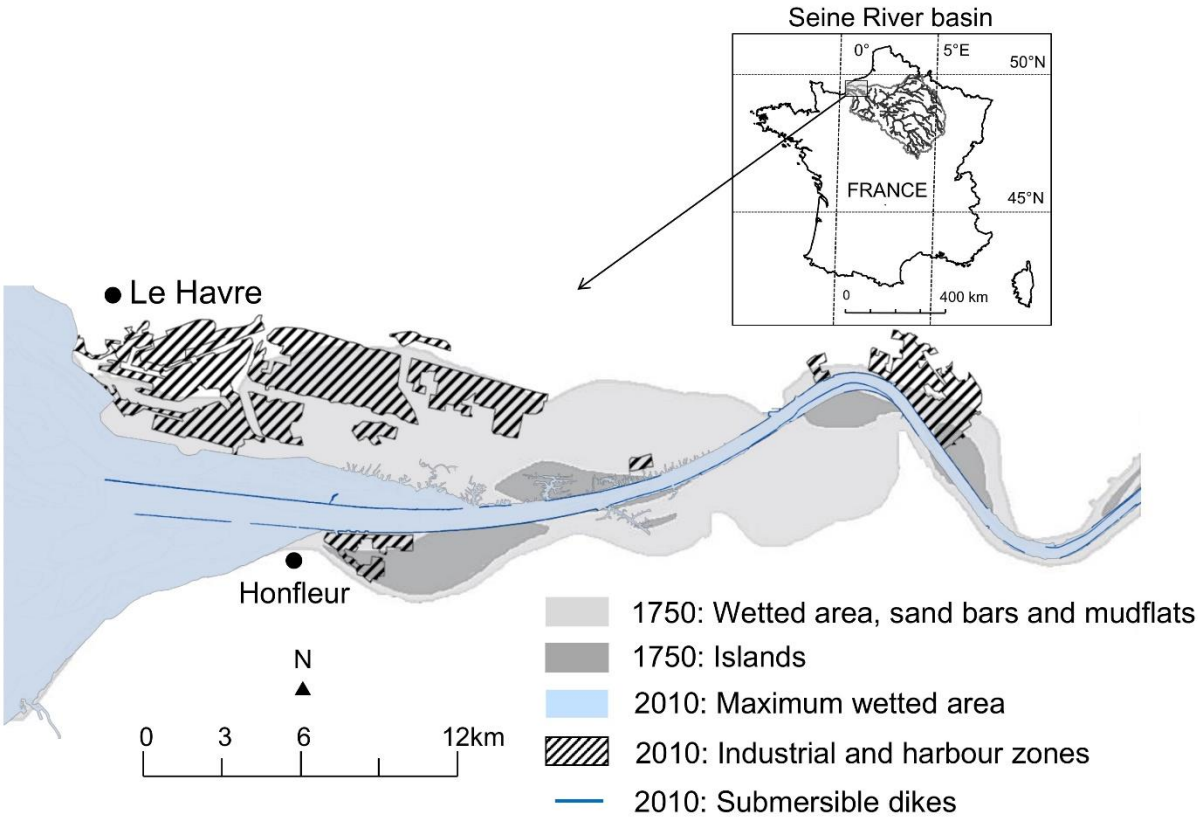

825
826

827 **Figure 3**

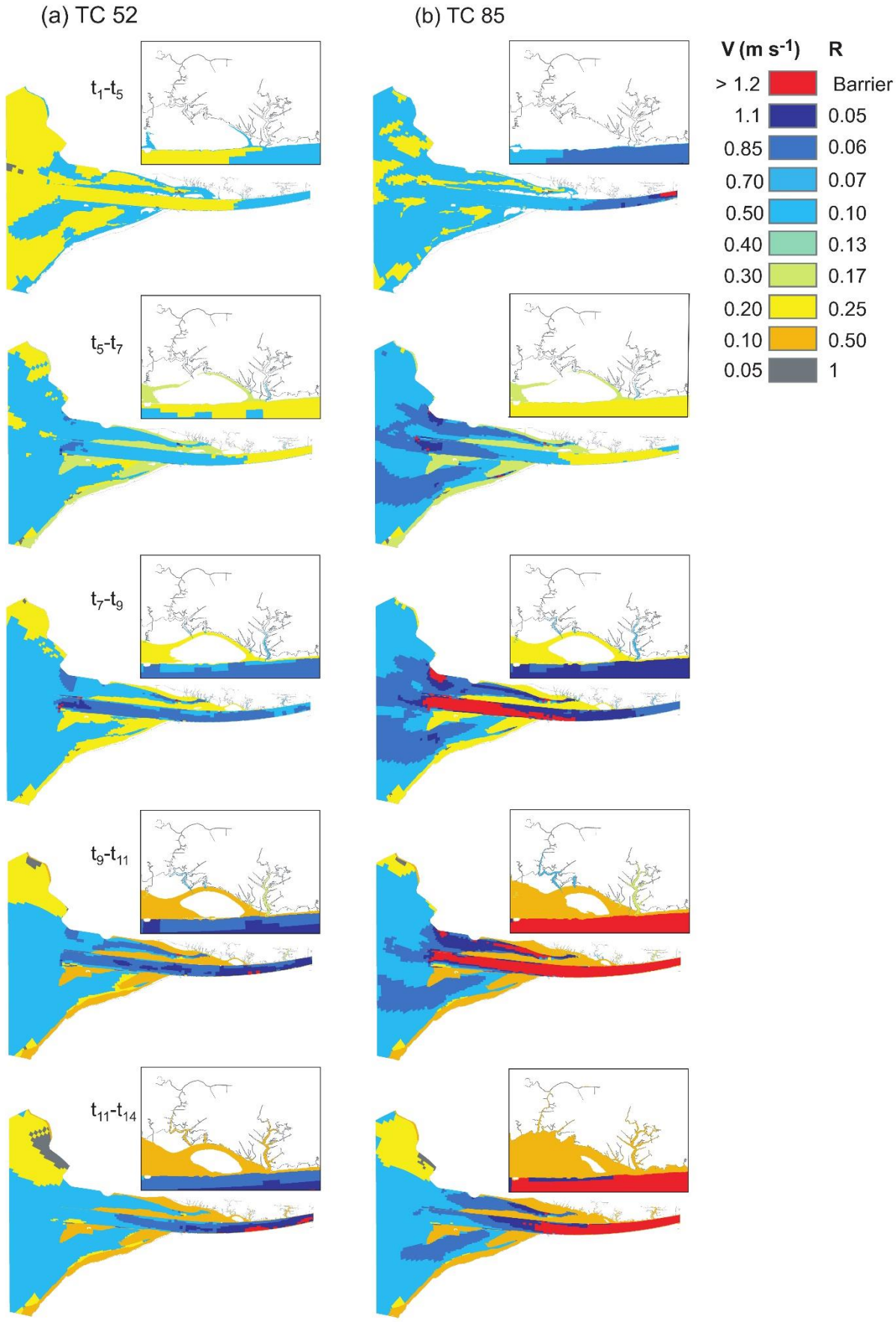

828

829 **Figure 4**

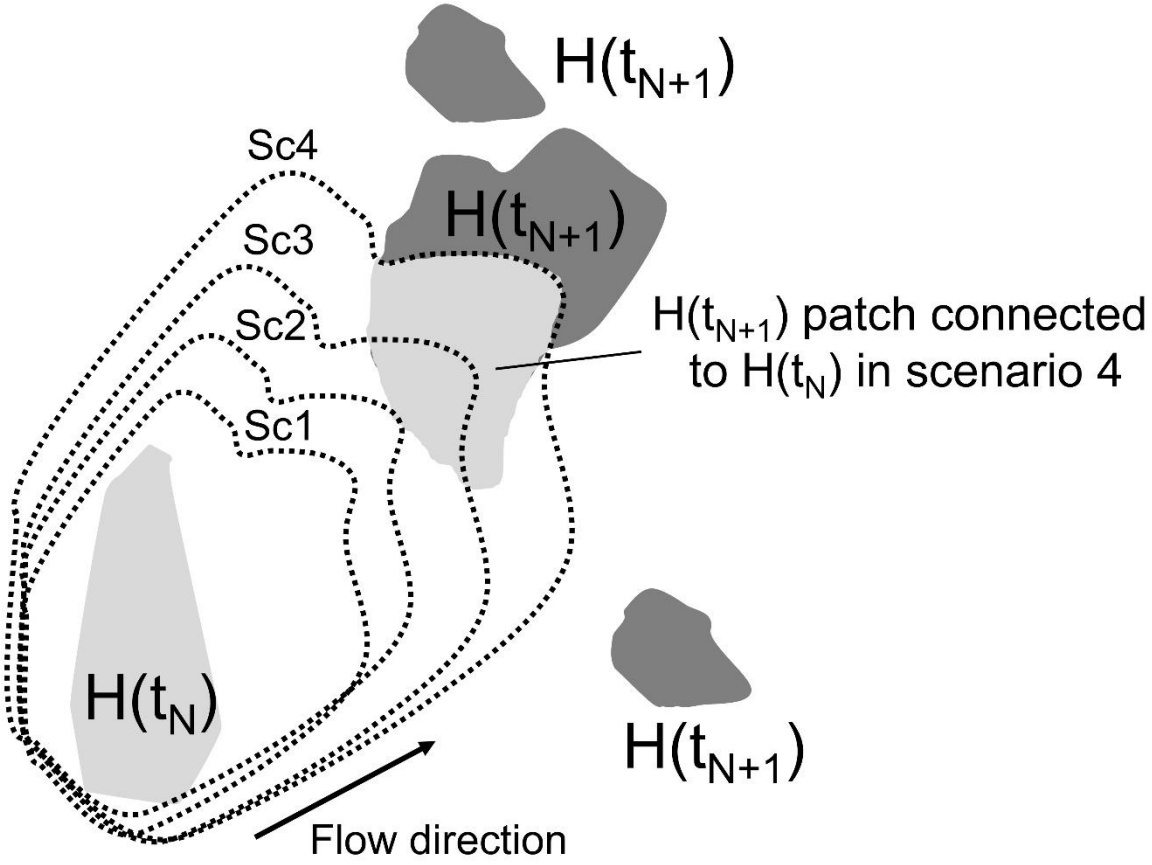

830
831
832

833 **Figure 5**

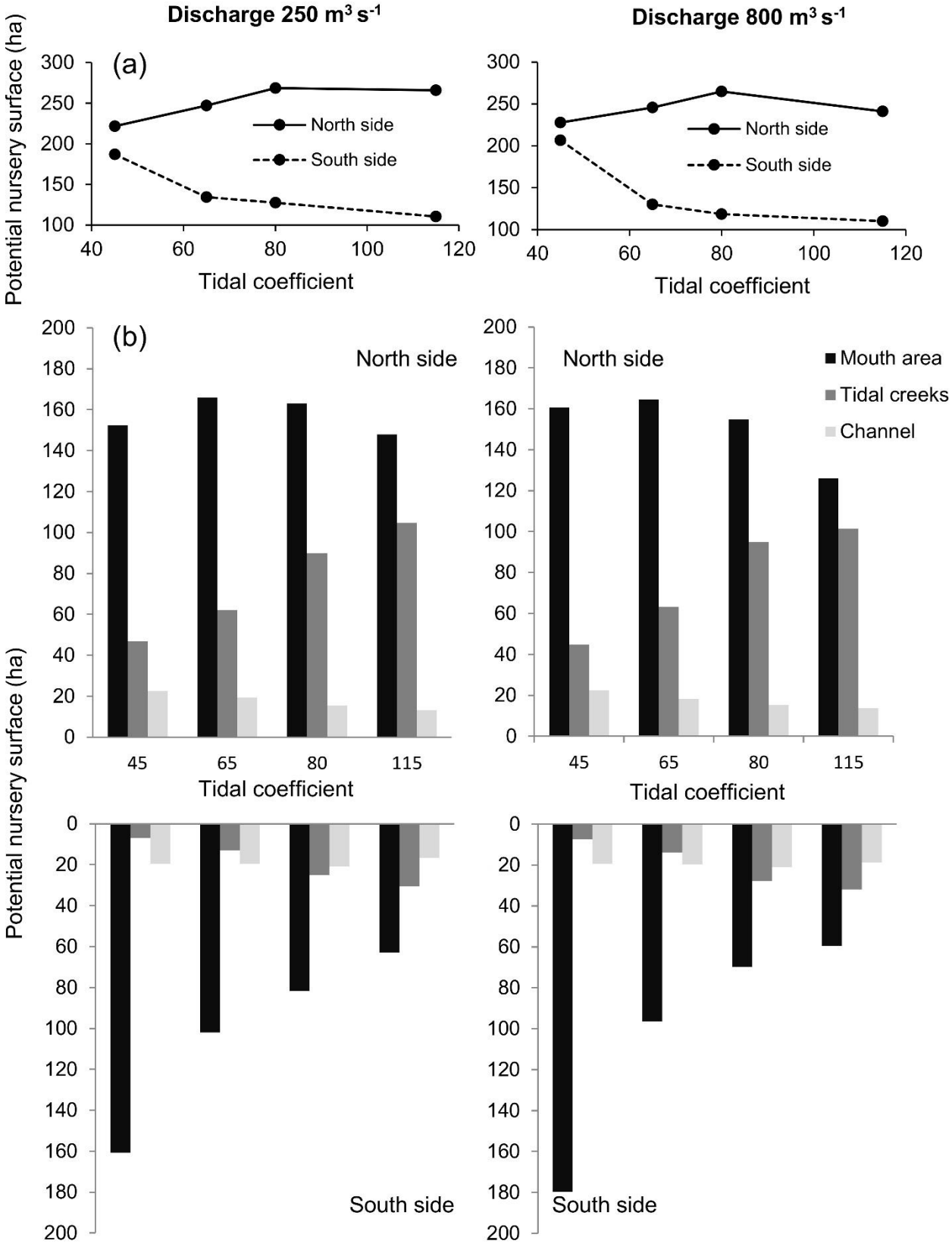

834

835

836 **Figure 6**

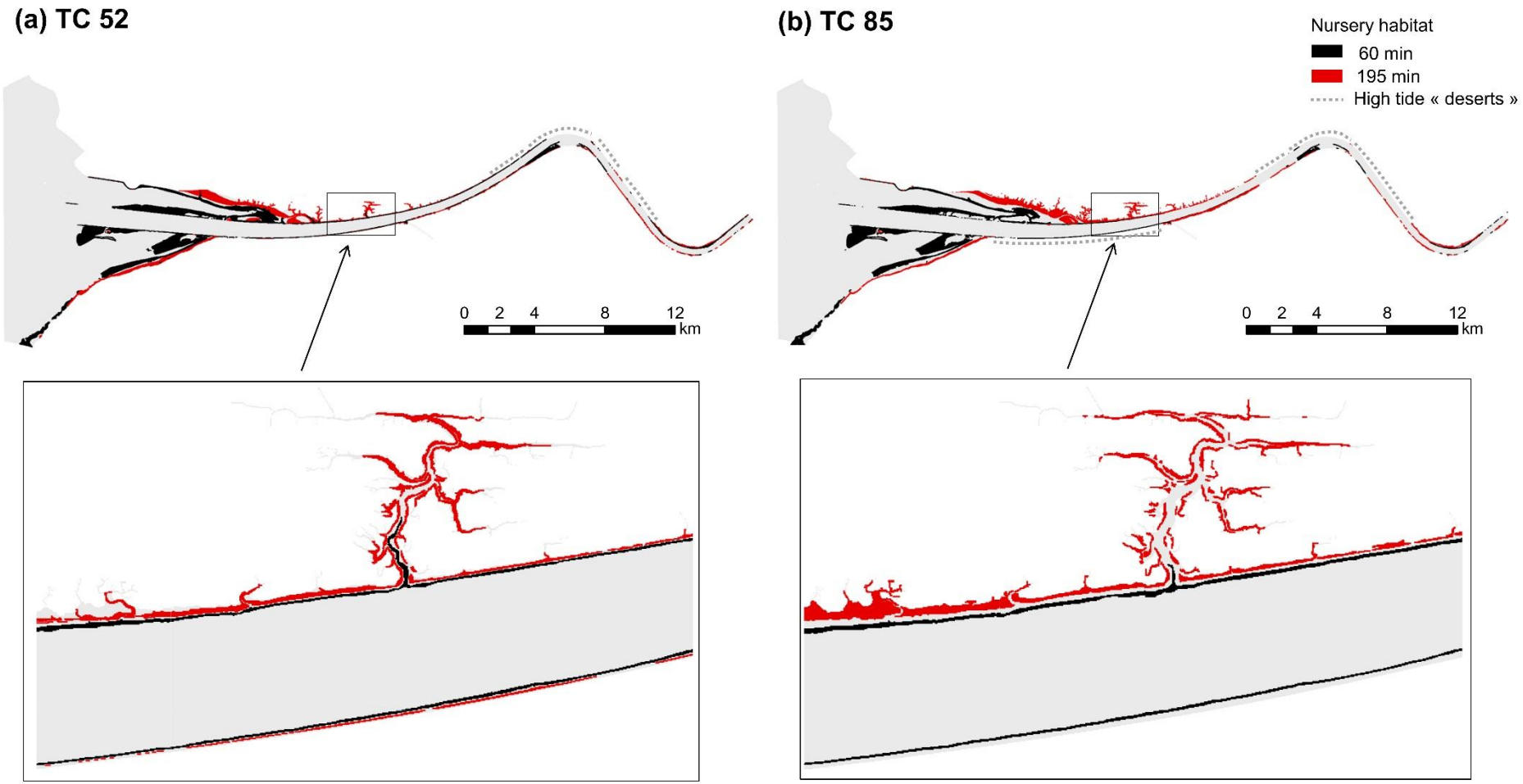

837
838
839

Figure 7

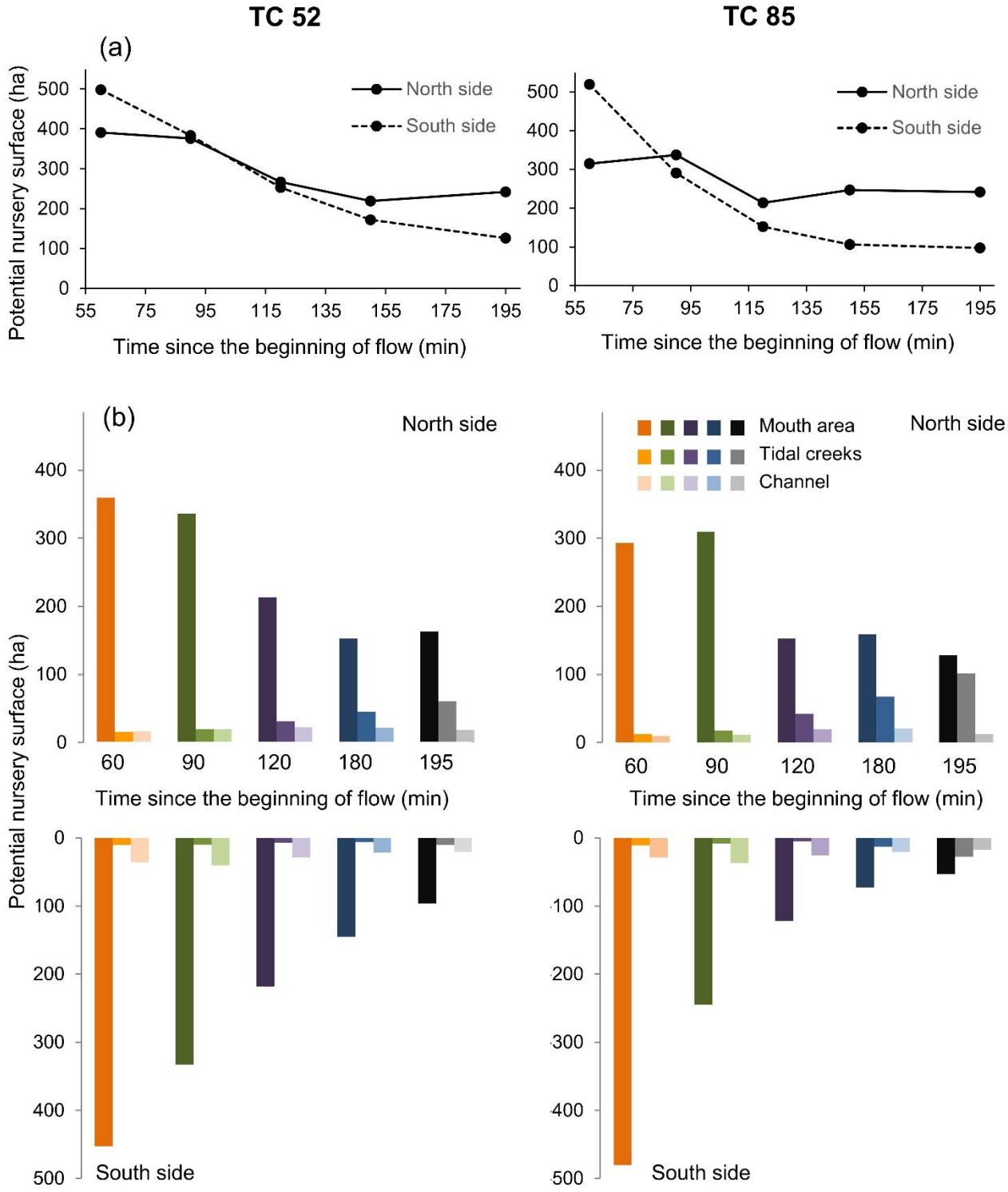
TC 52
TC 85
(a)
Potential nursery surface (ha)
North side
South side
Time since the beginning of flow (min)
(b)
Mouth area
Tidal creeks
Channel
60
90
120
180
195
0
100
200
300
400
500

Figure 8

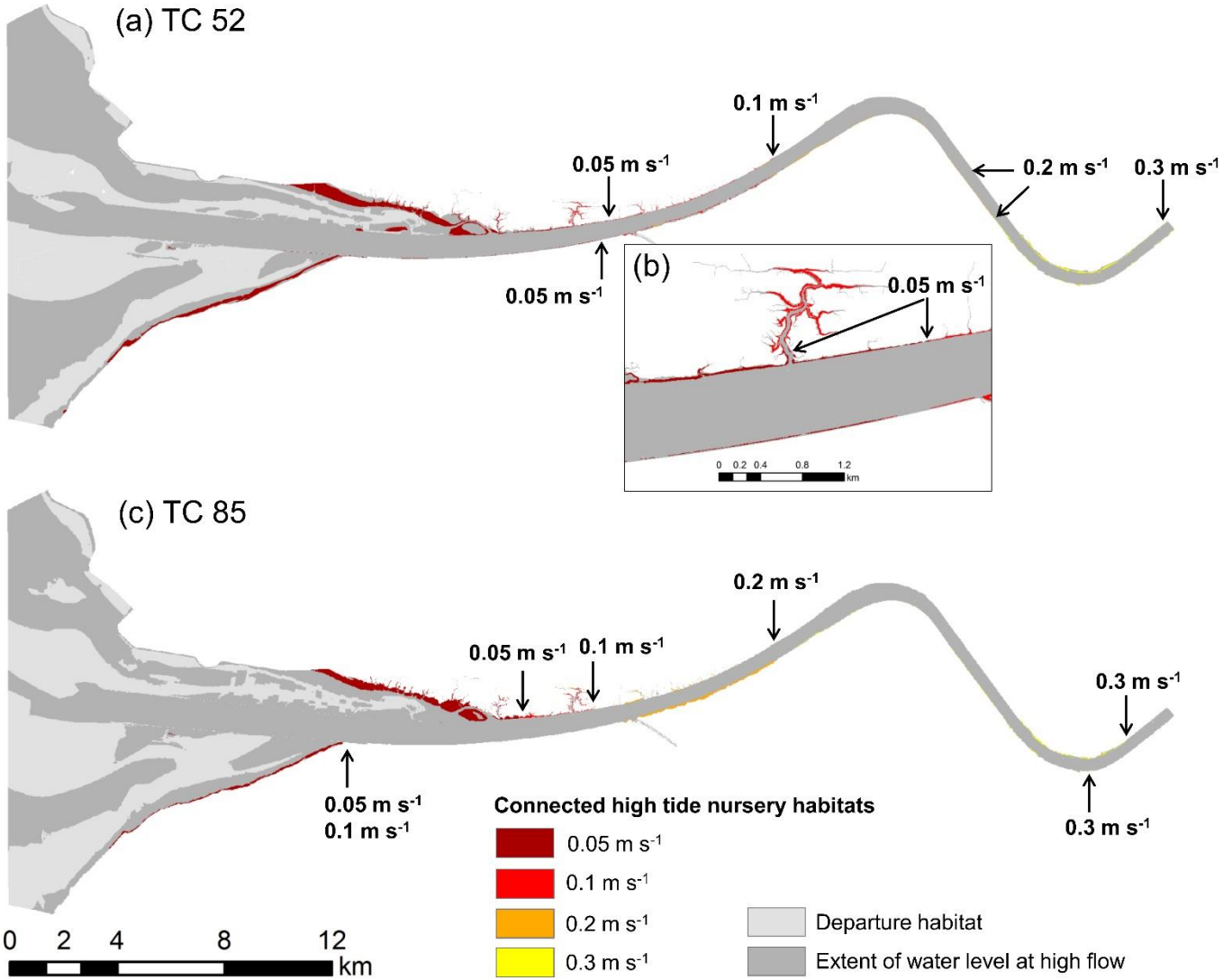
(a) TC 52
0.1 m s-1
0.05 m s-1
0.2 m s-1
0.3 m s-1
0.05 m s-1
(b)
0.05 m s-1
0 0.2 0.4 0.8 1.2
km
(c) TC 85
0.2 m s-1
0.05 m s-1
0.1 m s-1
0.3 m s-1
0.05 m s-1
0.1 m s-1
0.3 m s-1
Connected high tide nursery habitats
0.05 m s-1
0.1 m s-1
0.2 m s-1
0.3 m s-1
Departure habitat
Extent of water level at high flow
0 2 4 8 12
km

Figure 9

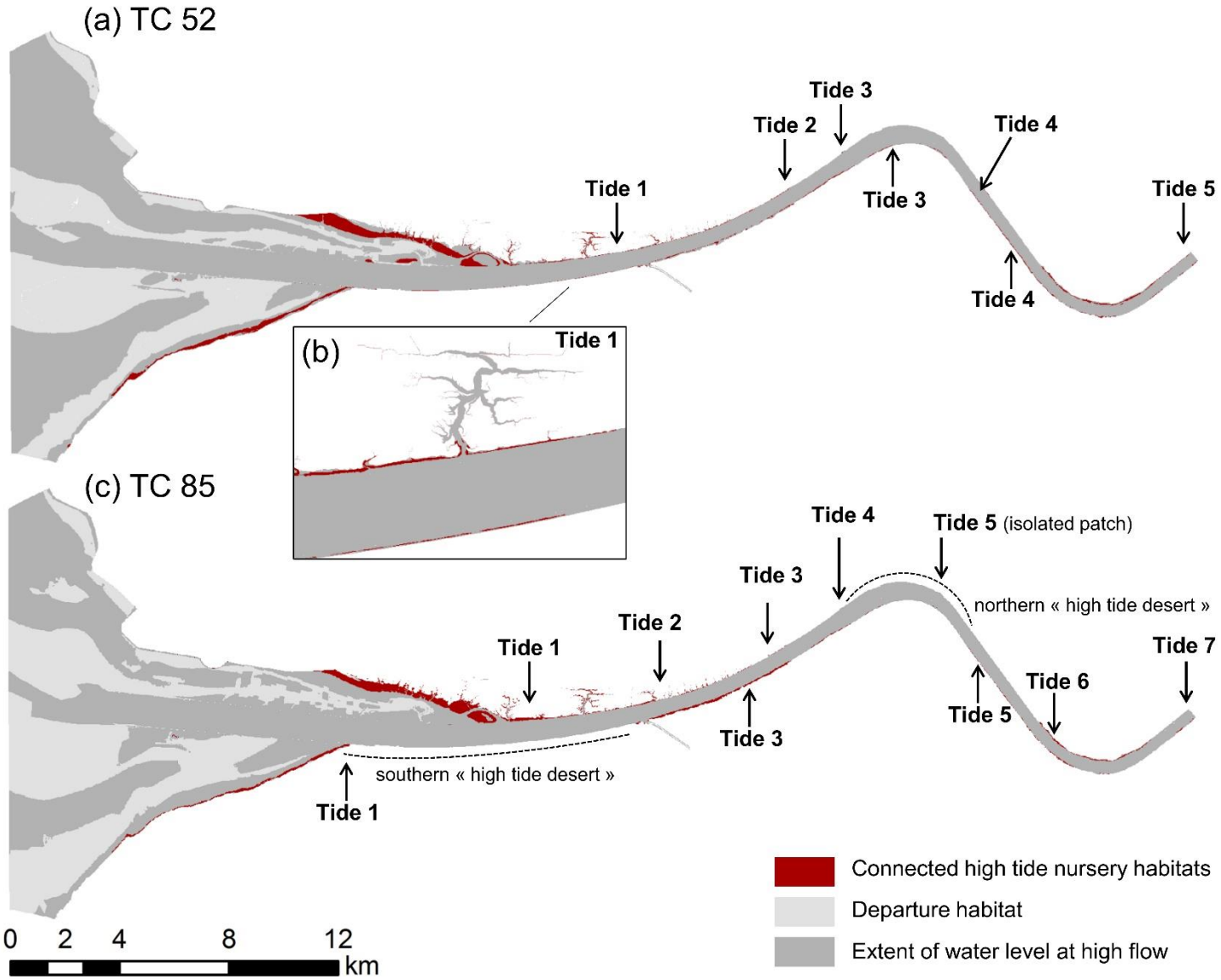
(a) TC 52
Tide 1
Tide 2
Tide 3
Tide 3
Tide 4
Tide 4
Tide 5
(b)
Tide 1
(c) TC 85
Tide 1
Tide 2
Tide 3
Tide 3
Tide 4
Tide 5 (isolated patch)
northern « high tide desert »
Tide 5
Tide 6
Tide 7
Tide 1
southern « high tide desert »
0 2 4 8 12
km
Connected high tide nursery habitats
Departure habitat
Extent of water level at high flow